PRAMANA
— journal of
physics

Vol. 75, No. 3
September 2010
pp. 523–536

Collision frequency of Lennard–Jones fluids at high densities by equilibrium molecular dynamics simulation

G A ADEBAYO[1,4,*], B C ANUSIONWU[3], A N NJAH[1], O J ADENIRAN[2], B MATHEW[1] and R S SUNMONU[1]

[1]Department of Physics, University of Agriculture, PMB 2240 Abeokuta, Nigeria
[2]Department of Mathematics, University of Agriculture, PMB 2240, Abeokuta, Nigeria
[3]Department of Physics, Federal University of Technology, Owerri, Nigeria
[4]The Abdus Salam International Centre for Theoretical Physics, Strada Costiera 11, I-34014 Trieste, Italy
[*]Corresponding author. E-mail: gadebayo@ictp.it

MS received 21 January 2010; revised 25 March 2010; accepted 6 April 2010

Abstract. Detailed classical molecular dynamics simulation of transport coefficients and collision frequencies at high densities in rare gases are presented in this paper with a view to investigate the likely cause of discrepancy between theory and experiments. The results, when compared with experiments, showed an underestimation of the viscosity calculated through the Green–Kubo formalism, but the results are in agreement with some other calculations performed by other groups. The origin of the underestimation was considered in the present work. Analyses of the transport coefficients showed a very high collision frequency which suggested that an atom might spend much less time in the neighbourhood of the fields of force of another atom. The distribution of atoms in the systems adjusts itself to a nearly Maxwellian type that resulted in a locally and temporarily slowly varying temperature. We showed that during collision, the time spent by an atom in the fields of force of other atoms is so small compared with its relaxation time, leading to a possible reduction in local velocity autocorrelation between atoms.

Keywords. Viscosity; diffusion; molecular dynamics; theory of simple liquids.

PACS Nos 51.20.+d; 61.20.-p; 61.20.Gy; 61.20.Ja; 65.20.De; 66.20.-d

1. Introduction

From early 1980s, computer simulation methods have been important and powerful tools in physics and other related disciplines [1–5]. Molecular dynamics (MD) simulation therefore, has become an essential numerical technique for the study of liquids and other systems at microscopic level. It is a robust way of calculation and the results obtained from MD simulations are generally exact. Classical MD simulations rely on Newton's equation of motion, integrations of which lead to information on static and dynamic behaviour of a system. In most MD simulations,

(shear) viscosity appears to be one of the most calculated properties and since the early days of the development of MD simulation, a number of methods have been developed and used successfully to calculate this important transport property in either equilibrium MD or non-equilibrium MD simulation. Gosling *et al* [6] adapted the momentum fluctuations method in their periodic perturbation approach to calculate the shear viscosity, and the same method was adopted in the work of Ciccotti *et al* [7]. Evans and Morriss employed the imposition of a linear velocity profile [8] in a simulation box with a view to accurately determine the viscosity. Other methods for calculating the shear viscosity can be found in [9,10].

Many authors have investigated the density dependence of the viscosity or the efficiencies of various interaction potentials used in calculations involving viscosity of rare gases. Marcelli and co-workers [11] investigated the shear viscosity for two-body and three-body potentials for non-equilibrium MD (NEMD). According to the authors, the three-body potential alters the magnitude of pressure, energy and viscosity profiles. Self-diffusion coefficients of four rare gases were determined by Fernandez *et al* [12] in equilibrium MD (EMD). Further, the shear and bulk viscosities were determined by the same workers. The agreements between their work and other theoretical calculations led to the conclusion that the available experimental data for bulk viscosity are inaccurate [13]. The density variation of the viscosity in a rare gas was determined by Mountain [14] among others. He showed that a semiclassical pair potential which accurately reproduced the low-density transport properties of xenon gas did not accurately generate the profile over a wider range of temperature and density. Very recently, Ciccotti and co-workers [15] reported their NEMD calculations of bulk viscosity using a Lennard–Jones model potential at triple point, and their results showed that linear response theory could not account adequately for the discrepancy between theory and experiments.

In this work, we attempt to find out the origin of this disparity between numerical and experimental results on the (shear) viscosity of rare gases and see if it has to do with the potential model or rather, a reduction in local correlations between the atoms in rare gases at high densities is responsible for the discrepancy. Several EMD simulations were carried out to determine the (shear) viscosity and other transport properties; comprehensive analyses of the shear viscosity based on relaxation time theory were carried out in order to estimate the level of deviation from experimental results. Our work is organized in the following order: Section 1 gives a brief introduction of the subject matter, in §2, the methods used are outlined with appropriate equations and theory. Findings of the present work are provided in §3, while in §4 concluding remarks are outlined.

2. Theoretical background and simulation technique

2.1 *Time spent in the fields of force*

In a system of interacting particles, we learnt from kinetic theory that the motion of two particles of masses m_1 and m_2 with velocities v_1 and v_2 respectively can be defined in terms of their centre of mass by the equation [16–19]

$$v' = \frac{m_1 v_1 + m_2 v_2}{m_1 + m_2}, \tag{1}$$

where the relative velocity is given as

$$v_{\mathrm{R}} = v_2 - v_1. \tag{2}$$

Since no external forces act on the particles, it is right to assume that v' remains constant during motion as well as when the particles collide. Therefore, the total kinetic energy can be written as

$$\frac{1}{2}m_1 v_1^2 + \frac{1}{2}m_2 v_2^2 = \frac{1}{2}(m_1 + m_2)v'^2 + \frac{1}{2}m^* v_{\mathrm{R}}^2. \tag{3}$$

Here, m^* is the effective mass written as

$$m^* = \frac{m_1 m_2}{m_1 + m_2}. \tag{4}$$

We must notice that the total kinetic energy is in two parts, namely, the kinetic energy of the two masses $(m_1 + m_2)$. This part remains constant throughout the whole motion. The second part has to do with the mass m^* moving with velocity v_{R}. The implication of the above statement is that, only the second part of the night-band side of eq. (4) is affected in collision. Now, if we consider an elastic collision, the total kinetic energy before and after collision should be the same. It therefore means that the elastic collision only changes the angle between v' and v_{R} without affecting the magnitudes of both velocities. An inelastic collision however will cause an increase in kinetic energy as energy is transferred between degrees of freedom during collision. The rate of energy transfer will be inversely proportional to the number of collisions a particle experiences per second. This is also true for the density, and in a way, it can be said that relaxation time is density dependent. The mean one-dimensional relative velocity $v_{1\mathrm{R}}$ can be written as

$$v_{1\mathrm{R}} = \sqrt{\frac{KT}{2\pi m^*}}. \tag{5}$$

Incoming particles are reflected either inelastically or elastically and we can write the fraction of the particles (with m_1) reflected inelastically after moving from position j to h as [18] $K_{j\to h}(v_{\mathrm{R}})^{-1}$. Also, the fraction of particles (with m_1) reflected elastically per unit time will be $Q_{\mathrm{el}} v_{\mathrm{R}} N_1$, where Q_{el} is the elastic cross-section and N_1 is the number of particles m_1. When elastic collisions are only a small fraction of the total collisions, we can write

$$Q_{\mathrm{inel}} v_{\mathrm{R}} N_1 = \frac{1}{\tau} = \Omega, \tag{6}$$

where Q_{inel} is the inelastic cross-section and τ is defined as the average time interval between collisions. Obviously, relaxation time will give rise to the rate at which deviations from equilibrium dies out. This could be seen if we consider a situation in which the time spent (duration of collision) by a particle in the neighbourhood of another is defined as

$$\tau_{\mathrm{dur}} = \frac{\sigma}{|v_{\mathrm{av}}|}, \tag{7}$$

where σ is the diameter of the particle and $v_{\rm av}$ its average speed. There could be a second situation in which the particles adjust to a nearly Maxwellian distribution which results in slowly varying temperature. The redistribution will take time $\tau_{\rm bet}$ between collision

$$\tau_{\rm bet} = \frac{\lambda}{|v_{\rm av}|}, \tag{8}$$

where λ is the mean free path. Furthermore, there could be a macroscopic adjustment to the true equilibrium with time $\tau_{\rm mac}$ given as

$$\tau_{\rm mac} = \frac{L^2}{\lambda^2}\tau_{\rm bet}, \tag{9}$$

where L is the length of the central simulation box. We see directly from eq. (9) that

$$\tau_{\rm mac} \approx \frac{L^2}{\lambda|v_{\rm av}|} \tag{10}$$

or that

$$\tau_{\rm mac} \approx \frac{L^2}{\lambda\sigma}\tau_{\rm dur}. \tag{11}$$

One needs to realize that at atmospheric pressure, the mean free path of a molecule in a gas is some hundreds of times its diameter, i.e.

$$\sigma \ll \lambda \tag{12}$$

and that the ratio of the macroscopic time to the duration time can be written as

$$\frac{\tau_{\rm mac}}{\tau_{\rm dur}} = \frac{L^2}{\lambda^2}\frac{\tau_{\rm bet}}{\sigma}v_{\rm av}. \tag{13}$$

Many of the equations above will be used in our analyses of the result obtained in the present simulation.

2.2 *Green–Kubo formalism for transport coefficients and relaxation collisions*

In hydrodynamics transport coefficient calculations, usually, linear response theory or the Onsager regression hypothesis leads to the Green–Kubo method. If the Onsager hypothesis is employed, we see that in a system at equilibrium, the fluctuations induced by thermal processes decay at long times in the same manner as in hydrodynamics distributions at macroscopic level. These transport coefficients are calculated as integrals of time-correlation functions of some quantities [20,21], and the shear viscosity of a system is its resistance to flow (resistance to shear forces) and it is sometimes related to the momentum transport under the influence of velocity gradients. Particularly, the off-diagonal stress tensor σ^{xy} auto-correlation function is used to determine this transport coefficient [22]:

$$\eta = \frac{1}{VK_{\mathrm{B}}T}\int_0^\infty \langle \sigma^{xy}(t)\cdot\sigma^{xy}(0)\rangle \,\mathrm{d}t. \tag{14}$$

Here, the integration is performed off the diagonal elements of the stress tensor, V is the volume and K_{B} denotes Boltzmann's constant. The stress tensor is written as the (x–y plane) shear stress

$$\sum_{i=1}^{N} m_i v_i^x v_i^y - \sum_{i=1}^{N}\sum_{j>i}^{N} r_{ij}^x \frac{\partial V(r_{ij})}{\partial r_{ij}^y}. \tag{15}$$

Following the idea suggested by Visscher [23], we can write the macroscopic decay for the mean free path in relaxation equation as

$$\dot{\lambda} = \frac{\mathrm{d}\lambda}{\mathrm{d}t} = -\Omega\lambda. \tag{16}$$

Asymptotically, ($t \to \infty$), averaging λ for the equilibrium time correlation function will give

$$\left(\frac{\mathrm{d}}{\mathrm{d}t}\right)\langle\lambda(t)\cdot\lambda(0)\rangle = -\Omega\,\langle\lambda(t)\cdot\lambda(0)\rangle\,. \tag{17}$$

This then means

$$\Omega = -\lim_{t\to\infty}\langle\dot{\lambda}(t)\cdot\lambda(0)\rangle/\langle\lambda(t)\cdot\lambda(0)\rangle. \tag{18}$$

Equation (18) provides a self-consistence route or a possible crosscheck of the relaxation time obtained from simulation using eq. (26). The bulk viscosity is calculated from the product of the pressure and volume combined with the stress tensor σ^{xx}

$$\eta_{\mathrm{bulk}} = \frac{1}{VK_{\mathrm{B}}T}\int_0^\infty \langle(\sigma^{xx}(t) - pV(t))\cdot(\sigma^{xx}(0) - pV(0))\rangle \tag{19}$$

and similarly,

$$\sigma^{xx} = \sum_{i=1}^{N} m_i v_i^x v_i^x - \sum_{i=1}^{N}\sum_{j>i}^{N} r_{ij}^x \frac{\partial V(r_{ij})}{\partial r_{ij}^x}. \tag{20}$$

In the above equations, $\langle\cdots\rangle$ denotes an ensemble average, i and j stand for the indices of particles i and j respectively, while the superscripts x and y denote the vector component of particle velocity v_i.

2.3 *The potential model and simulation technique*

The Lennard–Jones (LJ) pair potential was shown to work very well for rare gases [24–28]. It has also been used extensively to calculate the transport properties of various systems [29–35]. Schwartz and co-workers [36] and Grad [37] however

have shown that it is very difficult to determine the inelastic scattering of such a potential. It is not clear if this is due to the deficiency in the potential or to the constancy in the kinetic energy due to $m_1 + m_2$ as mentioned earlier.

The pair potential used in the present study is of the form

$$V(r_{i,j}) = 4\epsilon \sum_{i}^{N} \sum_{j \neq i}^{N} \left[\left(\frac{\sigma}{r_{i,j}} \right)^{12} - \left(\frac{\sigma}{r_{i,j}} \right)^{6} \right], \tag{21}$$

where $r_{i,j}$ is the distance between two interacting particles i and j. Here, the sums include all intermolecular pairs, whereas dispersion and overlap interactions are neglected. Simulations were performed at high densities and temperatures by inserting over 864 particles in a central simulation box and periodic boundary conditions were set. The parameters of the Lennard–Jones potential are given in table 1 and are obtained based on the total energy of a crystal [38]:

$$\Phi = \frac{1}{2} 4N\epsilon \left[\sum_{j} \left(\frac{\sigma}{\rho_{ij} r_N} \right)^{12} - \sum_{j} \left(\frac{\sigma}{\rho_{ij} r_N} \right)^{6} \right]. \tag{22}$$

Here, $\rho_{ij} r_N$ is the distance between a reference atom i and another atom j in terms of the distance of the nearest neighbour. The nearest neighbour will therfore contribute most of the interaction energy so that

$$\Phi = \frac{1}{2} 4N\epsilon c_n \left[\left(\frac{\sigma}{r_N} \right)^{12} - \left(\frac{\sigma}{r_N} \right)^{6} \right], \tag{23}$$

where c_n is the coordination number of the coresponding crystal and r_N is the equilibrium distance. The reduced units used here are given elsewhere [5]. At each run, a total time of $\frac{1}{3} t_{\mathrm{tot}}$ was used for equilibration. This is done to allow the initial crystal configuration to melt to a liquid state. Here, t_{tot} is the total simulation time. We have employed the microcanonical ensemble MD algorithm and several simulations were performed at a total of 17 states with temperatures ranging from 91 to 473 K and a low density of 0.37 mol/dm^3 and a high density of 2.95 mol/dm^3. The LJ potential was cut-off at a distance of $\frac{1}{2} L$, where L is the size of the central box. Ewald sum [4] technique was applied to correct for long-range interactions where necessary. In the integration of the equation of motion, the Verlet (leap frog) Algorithm [39] was employed with a time step of 0.004 in reduced unit.

Pair distribution function was used in the determination of all structural properties:

$$g(r) = \frac{V}{N} \left\langle \frac{\Delta N}{4\pi r^2 \Delta r} \right\rangle. \tag{24}$$

The above equation is an average over the time steps at equilibrium, where the volume of the simulation box with N particles is represented by V, while ΔN represents the number of particles in a shell within the region $r - \frac{\Delta r}{2}$ and $r + \frac{\Delta r}{2}$, where Δr is the thickness of the shell. Transport properties were calculated using the Green–Kubo (GK) formalism [5] and in few cases, calculations of transport

properties were performed based on Einstein relation to check the reliability of the GK equation. The Einstein relation can be written as [40]

$$D = \lim_{t\to\infty} \frac{\langle x^2(t)\rangle + \langle y^2(t)\rangle + \langle z^2(t)\rangle}{6t}. \tag{25}$$

A knowledge of the average velocity of particles in a gas allows to calculate the collision frequency f from which it may be possible to determine the collision time

$$f = 4\pi\rho r_{\max}^2 g(r_{\max}) \left(\frac{\pi K_{\mathrm{B}} T}{m}\right)^{1/2}, \tag{26}$$

where $r_{\max}$ is the position of the first peak in the pair distribution function and ρ is the homogenous density of the system, while only for convenience, we set K_{B} and m to unity. As far as we know, this is the first time that the time spent in the fields of force in combination with the relaxation time will be used to give an insight into the discrepancy between experiments and calculation results on shear (viscosity) of rare gases.

3. Results and discussion

In tables 2–4, we present at each temperature, the time spent in collision τ, obtained from the calculated collision frequency (eq. (28)) and the ratio τ/τ_{dur}. Except for argon, all calculations are based on conditions taken from [13,14]. The temperature dependence of the shear viscosity is highly pronounced in all the results, needless to say that the dependency shows an exponential form of the Arrheninus expression. Clearly, the above statement is true for the diffusion coefficient and we would like to add that, an onset of non-Arrheninus behaviour is not noticed over the temperature range used in our calculations.

Within the investigated temperature range, the time spent during collisions oscillate about a value. It is however not clear if this value will reduce or not with further increase in temperature over a wider range. The high collision frequency (low collision time) at high densities is a strong indication that particles have very little interactions. If we look at how much time (τ) a particle spent in the fields of force of another particle during collision, it is obvious (see table 5)

Table 1. The parameters of the Lennard–Jones potential.

System	ϵ (K)	σ (Å)
Argon	119.8	3.4
Krypton	167.0	3.7
Xenon	228.0	3.9

Table 2. Calculated time spent by a particle in the fields of force of other particles in argon at $\rho^* = 0.850$ near the triple point from our simulation.

T	τ (ps)$_{0.850}$
91	0.4
127	0.4
171	0.3

Table 3. Calculated time spent by a particle in the fields of force of another particle in krypton near the triple point and at $\rho^* = 0.105$ (2.95 mol/dm^3) from our simulation.

T	τ (ps)$_{0.105}$
281	0.43
314	0.43
344	0.43
405	0.42
473	0.41

Table 4. Calculated time spent by a particle in the fields of force of another particle during collision in xenon near the triple point at $\rho^* = 0.105$ from our simulation.

T	τ (ps)$_{0.105}$
281	0.45
314	0.43
344	0.43
405	0.42
473	0.41

Table 5. Comparison of time spent in the fields of force of another particle during collisions from simulation.

System	T (K)	$\lambda \times 10^{-8}$ m	Av. mol. sep. (m)	$\tau_\rho/\tau_{\rm dur}$	P (kPa)
Argon	91	0.701	1.533×10^{-9}	0.256	349
Argon	127	7.928	0.741×10^{-9}	0.304	4306
Argon	171	5.361	0.651×10^{-9}	0.022	8574
Krypton	281	1.286	1.985×10^{-9}	0.309	496
Krypton	314	1.021	1.838×10^{-9}	0.328	697
Krypton	344	0.982	1.815×10^{-9}	0.344	795
Krypton	405	1.419	2.051×10^{-9}	0.363	648
Krypton	473	2.934	2.613×10^{-9}	0.384	366
Xenon	281	0.510	1.510×10^{-9}	0.246	1126
Xenon	314	0.734	1.706×10^{-9}	0.249	873
Xenon	344	0.760	1.725×10^{-9}	0.260	925
Xenon	405	0.967	1.869×10^{-9}	0.276	857
Xenon	473	1.344	2.086×10^{-9}	0.290	719

that this time is much less than the normal time a particle is supposed to spend during collision ($\sigma/|v_{\rm av}|$). These values suggest a fast process in which there is a likelihood of reduction or destruction of correlation between particles and between velocity of the particles. To illustrate this fact, the mean free path or the average distance between collisions was determined in the simulations and in all the cases, it was discovered to be larger than the average molecular seperations in the systems. Furthermore, the ratio ($\lambda/|v_{\rm av}|$) implies (not shown here) a situation in which the distribution of particles after collision adjusts to a nearly Maxwellian distribution with a slowly varying temperature.

Necessary equation that enters the simulation can be derived by considering the diameter σ of a particle with an effective cross-section $\pi\sigma^2$. Using a circle of diameter 2σ to reperesent a particle's collision area and treating the target particles as point masses [41–44], in time t, the circle would sweep out a volume $\pi\sigma^2 v_{\rm av} t$, while the

number of collisions can be estimated from the number of gas particles N_{V} that are within this volume. Of course, the distance travelled by such a particle would be $v_{\mathrm{av}}t$. So we can write

$$\lambda = \frac{v_{\mathrm{av}}t}{\pi\sigma^2 v_{\mathrm{av}}tN_{\mathrm{V}}} \tag{27}$$

$$= \frac{\text{distance travelled}}{\text{volume of interaction} \times \text{number of particles per unit volume}} \tag{28}$$

$$= \frac{1}{\pi\sigma^2 N_{\mathrm{V}}}. \tag{29}$$

The above equation assumes that other particles are at rest. In order to correct for this situation, we introduce the average relative velocity v_{R} as

$$v_{\mathrm{R}} = \sqrt{2}v_{\mathrm{av}}. \tag{30}$$

By combining eqs (29) and (30) into eq. (27), the substitution of velocities results in

$$\lambda = \frac{1}{\sqrt{2}\pi\sigma^2 N_{\mathrm{V}}}. \tag{31}$$

By introducing Avogadro's number, an equation for λ in the simulation emerged:

$$\lambda = \frac{RT}{\sqrt{2}\pi\sigma^2 N_{\mathrm{A}}P}. \tag{32}$$

Here, N_{A} and P are Avogadro's number and the pressure respectively.

In figure 1, the plot of inverse of the collision frequency with temperature is shown in argon. Here, the temperature dependence of collision time is highlighted. As the temperature increases, there is a corresponding increase in collision frequency as a decrease in collision time is noticed. Although, this relationship is linear in the range studied, it is not sure whether the linearity extends over a large temperature range. Figure 2 shows the same plot in krypton, but for collision frequency vs. temperature over a wider range of temperatures; the dependency in this case is non-linear. Figure 3 shows the velocity autocorrelation function with respect to time step in argon at three different temperatures, and a perusal of the graph confirms the non-linearity of the shear viscosity with temperature as shown in figure 4. In figure 5, we present our results on viscosity in comparison with experiment, and it can be seen that there is a good agreement between simulation results from the present work and that of ref. [14] while, a large discrepancy is noticed between simulation results from the present work and that of ref. [50]. Viscardy and co-workers employed the Helfand–Moment (HM) method in the calculation of the shear viscosity, while Meier and co-workers used a generalized Einstein relation with flux (GEF) integration. A comparison between our calculations and others is presented in table 6. We have reasonable agreements within the range considered as it has been shown [51] for Lennard–Jones rare gases that the cut-off radius r_{c} actually affects the calculated properties even when correction terms are added.

We would like to stress that the discrepancy between numerical calculations and experiments may not be due to model potentials, but may be due to the fact that

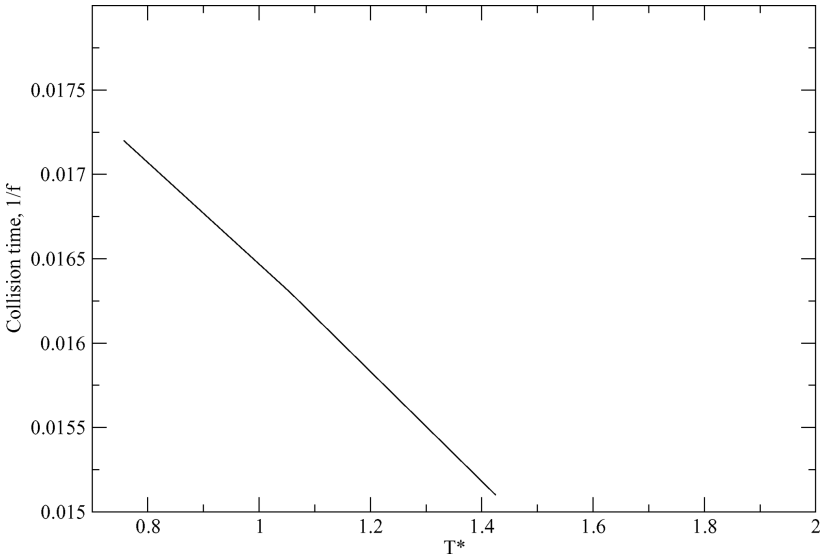

Figure 1. Relationship between time spent between collisions in argon at high density near the triple point.

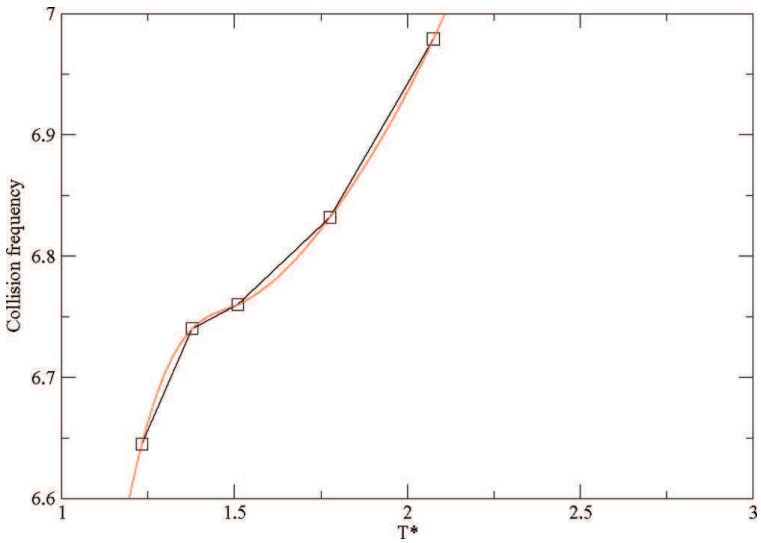

Figure 2. The collision frequency in krypton near the triple point at high density. The empty boxes are results from present simulation, continous line is obtained from cubic spline fit to simulation data.

an atom at high density and high temperature, an atom spend less time during collision with other atoms. This reduction in time could make atoms to have very little interactions which might have an effect on the velocity autocorrelation function and consequently on the values of (shear) viscosity.

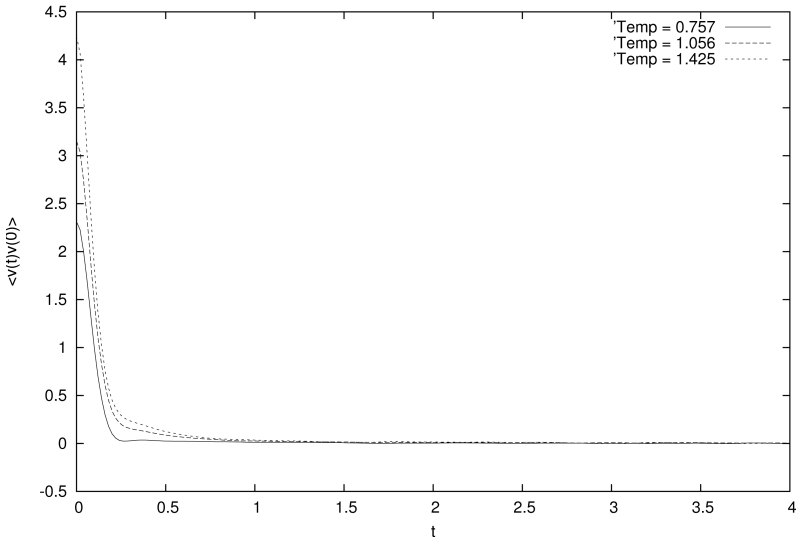

Figure 3. Velocity autocorrelation function with respect to time in argon at high density near the triple point.

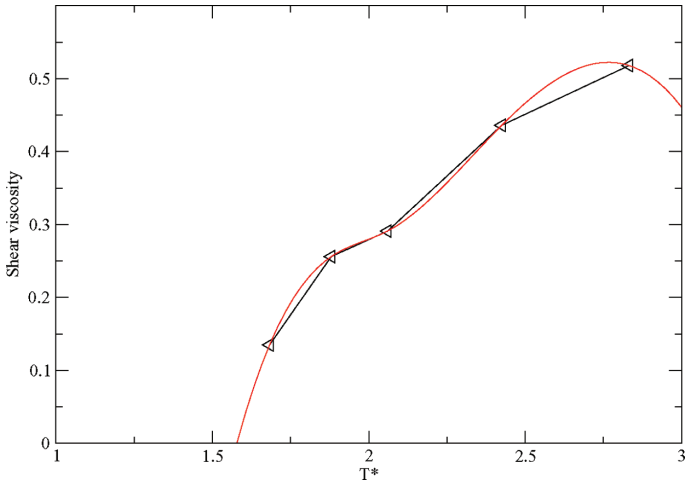

Figure 4. Calculated shear viscosity in krypton from simulation (triangles), the line is a spline fit to simulation result.

4. Conclusions

Extensive molecular dynamics simulations of rare gases were performed in this work in the temperature range 91 K $\leq T \leq$ 473 K and at various pressures to determine the shear viscosity and the bulk viscosity of these gases. Using kinetic theory, we were able to determine the collision frequency from which it was possible to obtain information on how much time an atom spent in the neighbourhood of another

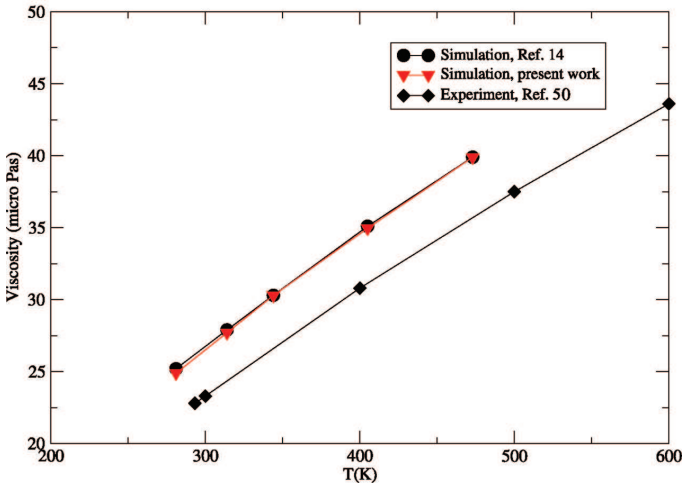

Figure 5. Calculated viscosity compared with other simulation and experiments.

Table 6. Comparison of shear and bulk viscosity results near the triple point.

Source	ρ^*	T^*	N	r_c^*	Method	η
Reference [47]	0.8442	0.73	500	2.5	GK	3.18
Reference [48]	0.8442	0.72	864	2.5	GK	3.20
Reference [49]	0.8442	0.72	864	2.5	GK	3.24
Reference [45]	0.8442	0.72	864	5.0	GEF	3.31
Reference [46]	0.8442	0.72	864	2.5	HM	3.25
Present work	0.8442	0.75	864	3.4	GK	3.24

atom during collision. We propose a reason for the discrepancy between numerical and experimental results on shear viscosity and bulk viscosity of Lennard–Jones fluids. The relaxation time and the actual time spent during collisions were used to determine how much time an atom spent in the fields of force of another atom during collision. It was discovered that the time spent in the fields of force of other atoms during collisions was actually a fraction of the actual time an atom should spend during collisions.

In rare gases, the shells are closed and when two particles approach each other, the Coulombic field of force between them decelerates or accelerates the particles as the case may be, and consequently, kinetic energy is transferred to the field from one of the colliding particles. Then the field transmits equivalent kinetic energy to the other particle, leading to action and reaction between the colliding particles. This process between the colliding particles is essentially caused by electrostatic fields of force, which are responsible for the Coulomb force.

The repulsion effect 'modifies or reduces' the velocity with which a particle approaches another particle before collision. The reduction in velocity can ultimately affect velocity autocorrelation function which can lead to lower values of shear

viscosity. We know that when two particles collide, electrons come very close and in the process, fields of force are created. It then means that any calculations of shear viscosity based on velocity autocorrelation function will usually give an underestimation of the true value of shear viscosity at high densities. One then must incorporate the effect of fields of force in such calculations.

Acknowledgement

The authors would like to express gratitude to Prof. R D Mountain for sending his data on xenon gas. GAA and BCA are grateful to the Abdus Salam ICTP for financial support and hospitality as Junior Associates of the ICTP.

References

[1] G Ciccotti and W G Hoover (Eds.), *Molecular dynamics simulation of statistical-mechanical systems* (North-Holland, Amsterdam, 1986)
[2] G Ciccotti and J F Ryckaert, *Comput. Phys. Rep.* **4**, 345 (1986)
[3] D W Heerman, *Computer simulations methods* (Springer-Verlag, Berlin, 1986)
[4] M P Allen and D J Tildesley, *Computer simulation of liquids* (Oxf. Univ. Press, Oxf., 1987)
[5] D Frenkel and B Smit, *Understanding molecular simulation: From algorithms to applications* (Academic Press, NY, 1996)
[6] E M Gosling, I R McDonald and K Singer, *Mol. Phys.* **26**, 1475 (1973)
[7] G Ciccotti, G Jacucci and I R McDonald, *Phys. Rev.* **A13**, 426 (1976)
[8] D J Evans and G P Morriss, *Phys. Rev.* **A30**, 1528 (1984)
[9] F Mueller-Plathe, *Phys. Rev.* **E59**, 4894 (1999)
[10] G Arya, E J Maginn and H Chang, *J. Chem. Phys.* **113**, 2079 (2000)
[11] G Marcelli, B D Todd and R J Sadus, *Fluid Phase Equilibria* **183**, 371 (2001)
[12] G A Fernandez, J Vrabec and H Hasse, *Int. J. Thermophys.* **25**, 175 (2004)
[13] G A Fernandez, J Vrabec and H Hasse, *Fluid Phase Equilibria* **221**, 157 (2004)
[14] R D Mountain, *Int. J. Thermophys.* **28**, 259 (2007)
[15] P L Palla, C Pierleone and G Ciccotti, *Phys. Rev.* **E78**, 021204 (2008)
[16] J Jeans, *An introduction to the kinetic theory of gases* (Cambridge Univ. Press, 1962)
[17] V Garzo and A Santos, *Kinetic theory of gases in shear flow* (Kluwer Acad. Publishers, 2003)
[18] D Sette (Ed.), *Dispersion and absorption of sound by molecular processes* (Acad. Press Inc., NY, 1963)
[19] S G Brush, *Kinetic theory* (Pergamon Press, 1966)
[20] R Kubo, *J. Phys. Soc. Jpn* **12**, 570 (1957)
[21] M S Green, *J. Chem. Phys.* **22**, 398 (1954)
[22] W A Steele, in: *Transport phenomena in fluids* edited by H J M Hanley (Marcel Dekker, New York and London, 1969)
[23] P B Visscher, *J. Chem. Phys.* **89**, 5137 (1988)
[24] L Verlet, *Phys. Rev.* **159**, 98 (1967)
[25] X J Chen, F Ercolessi, A C Levi and E Tosatti, *Surf. Sci.* **249**, 237 (1999)
[26] E M Bringa, *Nucl. Instrum. Methods Phys. Res.* **153**, 64 (1999)

[27] E S Landry, S Mikkilineni, M Paharia and A J H McGaughey, *J. Appl. Phys.* **102**, 124301 (2007)
[28] H Kaburaki, J Li, S Yip and H Kimizuka, *J. Appl. Phys.* **102**, 043514 (2007)
[29] S W Rutherford, D T Limmer, M G Smith and K G Honnell, *Polymer* **48**, 6719 (2007)
[30] S H Lee, *Bull. Korean Chem. Soc.* **29**, 641 (2008)
[31] A M Bazhenov and D M Heyes, *J. Chem. Phys.* **92**, 1106 (1990)
[32] J Lopez-Lemus and J Alejandre, *Mol. Phys.* **101**, 743 (2003)
[33] T Duren, F J Keil and N A Seaton, *Mol. Phys.* **100**, 3741 (2002)
[34] G A Fernandez, J Vrabec and H Hasse, *Fluid Phase Equilibria* **249**, 120 (2006)
[35] M F Pas and B J Zwolinski, *Mol. Phys.* **73**, 471 (1991)
[36] R N Schwartz, Z I Slawsky and K F Herzfeld, *J. Chem. Phys.* **20**, 1591 (1952)
[37] H Grad, *Handb. d. Phys.* **12**, 205 (1959)
[38] C Kittel, *Introduction to solid state physics* (Wiley, New York, 1975)
[39] R W Hockney and J W Eastwood, *Computer simulation using particles* (McGraw-Hill, New York, 1981)
[40] J P Hansen and I McDonald, *Theory of simple liquids* (Acad. Press, London, 1976)
[41] L B Loeb, *The kinetic theory of gases* (Courier Dover Publications, 2004)
[42] E Bloch and P A Smith, *The kinetic theory of gases* (Methuen & Co. Ltd., 1924)
[43] W Wilson, *A hundred years of physics*, READ BOOKS ISBN 140671075X, 9781406710755 (2007)
[44] A Mulero, *Theory and simulation of hard-sphere fluids and related systems* (Springer-Verlag, Berlin, Heidelberg, 2008)
[45] K Meier, A Laesecke and S Kabelac, *J. Chem. Phys.* **121**, 3671 (2004)
[46] S Viscardy, J Servantie and P Gaspard, *J. Chem. Phys.* **126**, 184512 (2007)
[47] M Schoen and C Hoeisel, *Mol. Phys.* **56**, 653 (1985)
[48] J J Erpenbeck, *Phys. Rev.* **A38**, 6255 (1988)
[49] M Ferrario, G Ciccotti, B L Holian and J P Ryckaert, *Phys. Rev.* **A44**, 6936 (1991)
[50] N B Vargaftik, *Tables on the thermophysical properties of liquids and gases* (Hemisphere Publ. Corp., NY, 1975)
[51] K V Tretiakov and S Scandolo, *J. Chem. Phys.* **120**, 3765 (2004)